J Electr Eng Technol.2016; 11(4): 878-888
http://dx.doi.org/10.5370/JEET.2016.11.4.878

ISSN(Print) 1975-0102
ISSN(Online) 2093-7423

Cogging Torque Reduction in Line Start Permanent Magnet Synchronous Motor

Hamidreza Behbahanifard * and Alireza Sadoughi†

Abstract – Cogging torque has a negative impact on the operation of permanent magnet machines by increasing torque ripple, speed ripple, acoustic noise and vibration. In this paper Magnet Shifting Method has been used as a tool to reduce the cogging torque in inset Line Start Permanent Magnet Synchronous Motor (LSPMSM). It has been shown that Magnet Shifting Method can effectively eliminate several lower-order harmonics of cogging torque. In order to implement the method, first the expression of cogging torque is studied based on the Fourier analysis. An analytical expression is then introduced based on Permanent Magnet Shifting to reduce cogging torque of LSPMS motors. The method is applied to some existing machine designs and their performances are obtained using Finite Element Analysis (FEA). The effect of magnet shifting on pole mmf (magneto motive force) distribution in air gap is discussed. The side effects of magnet shifting on back-EMF, core losses and torque profile distortion are taken into account in this investigation. Finally the experimental results on two prototypes 24 slot 4 pole inset LSPMS motors have been used to validate the theoretical analysis.

Keywords: Line Start Permanent Magnet Synchronous Motor (LSPMSM), Cogging torque, Magnet shifting, Torque ripple, Back EMF

1. Introduction

Studies have shown 30% to 40% of the generated worldwide electrical energy is being consumed by electric motors in industrial applications [1]. Environmental concerns and in particular the increasing acceleration of global warming due to emission of greenhouse gases from power stations has led to growing pressure on the manufacturers for producing higher efficiency electrical machines.

Among various types of electrical motors, small three phase induction motors are widely used in many industrial applications such as pumps and fans [2]. Small Induction Motors (IM) has relatively low operational efficiency and power factor, which has limited their application. Alternative options to the induction motors are the high efficiency Permanent Magnet (PM) motors. On the other hand a PM motor needs inverter for starting which is not economical for many single speed applications such as most fans, pumps and compressors. For economical and operational reasons any new motor should be capable of directly replacing the existing induction motor. Therefore a line start permanent magnet synchronous motor is a suitable alternate choice.

Synchronous motors possess many attractive features including simple structure, high efficiency, low loss, high power factor, small volume and light weight. However, their operations are negatively impacted by cogging torque [3, 4]. Cogging torque reduces the torque quality by producing undesired vibration and mechanical noise, which seriously impact the machine performance especially in low speed and direct drive applications [5]. Large cogging torque has also caused difficulties during motor start-up [6]. Cogging torque is caused by the interaction between the magnets mounted on the rotor and the stator anisotropy due to stator slotting. Cogging torque produces zero net work, but it acts as a disturbance superimposed on the electromagnetic torque generated during machine operation. As a result minimizing the induced ripple is of great importance in the design of PM machines [7].

Researchers have investigated different methods for reducing the cogging torque. Slot skewing [4] and [8], magnet skewing [9], auxiliary slots or teeth [10] and [11], pole-arc optimization [12] to [15], slot or tooth paring [16], magnet segmentation [17] and [18], magnet shifting and shaping [9, 13] to [15, 19] and [21] are examples of the solutions have been proposed in the literature for reducing cogging torque. Although these techniques are successful in reducing the undesired cogging torque, but they can also reduce the desired mutual torques. This along with the higher manufacturing cost, associated with the generally more complex machine designs, are the two main trades offs in reducing cogging torque [20]. The Magnet Shifting Method is shown to be very effective in reducing cogging torque. In this method the magnetic poles are shifted in

† Corresponding Author: Dept. of Electrical and Avionics Engineering, Malek Ashtar University of Technology, Iran. (sadoughi@mut-es.ac.ir)
* Dept. of Electrical and Avionics Engineering, Malek Ashtar University of Technology, Iran. (h-behbahani@mut-es.ac.ir)
Received: February 9, 2015; Accepted: December 22, 2015

such a way to set the magnetic field distribution to be asymmetric. This shift creates a compensation effect and will reduce the cogging torque.

The main purpose of this article is to reduce the cogging torque in inset LSPMS motors by method of magnet shifting. First the analytical expression derived by Fourier series analysis is reviewed and then the principle of magnet shifting method will be implemented. The method will be confirmed by the finite element analysis of a four pole inset LSPMS motor. The side effects on magnetic fields harmonics, back EMF, core loss and electromagnetic torque are all taken into account. Finally, the experimental results of two prototypes 24 slot 4 pole inset LSPMS motors are used to validate the theoretical analysis.

2. Cogging Torque Analysis

The cogging torque is caused by interactions between the permanent magnets mounted on the rotor and the anisotropy due to stator slots [4]. Because of this anisotropy the magnetic field energy changes during the rotation and a torque is produced which can be expressed as:

$$T_{cog} = -\frac{\partial W_f}{\partial \theta} \tag{1}$$

The associated filed energy in Eq. (1) can be obtained from equation:

$$W_f = \frac{1}{2\mu_0}\int B^2\, dv \tag{2}$$

In which B is the flux density and can be defined as:

$$B = \Lambda . F \tag{3}$$

Where Λ is the permeance and can be calculated as:

$$\Lambda = \frac{\mu_0}{L_{gap}} \tag{4}$$

In the above μ_0 is the vacuum permeability, L_{gap} represents the magnet to slot gap and F is the magneto motive force (mmf) generated by the magnets. Stator winding slots cause periodical variation of L_{gap} along the angular position as shown in Fig. 1 [15]. The periodical air gap reluctance causes the cogging torque to be periodic so the resulting cogging torque can be described using a Fourier series shown below:

$$T_{cog} = \sum_{k=1}^{\infty} T_{mk} \sin(mk\theta) \tag{5}$$

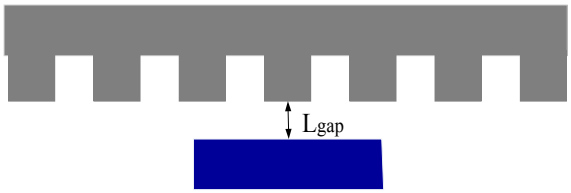

Fig. 1. Periodical variation of L_{gap}

Where m is the least common multiple of the number of stator slots (N_s) and the number of poles (N_p), k is an integer and T_{mk} is the Fourier coefficient. The common used assumptions suppose that the end effect and the iron saturation are negligible and therefore the superposition rule can be used. By using superposition principle the total cogging torque can be obtained by sum of the contributions from each magnet. Therefore in machines where the rotor and stator contain magnets and winding slots, which are periodically distributed in angle, the cogging torque increases through an additive effect. This is due to the fact that each magnet has the same relative position with respect to the stator slots so the torque from each magnet is in phase with other magnets and as a result the harmonic components of each magnet are added together.

To illustrate the influence of pole numbers and pole position on the cogging torque a 4 pole 24 stator slot inset LSPMS motor is selected for investigation. As shown in Fig. 2, motors with different pole numbers (one, two, four and also one shifted magnet) are taken into account.

The simulation results are presented in Fig. 3. As shown the results verify that the total cogging torque can be obtained as the sum of contributions from each magnet. In addition the results also show that the phase of cogging torque of a magnet changes when the magnet is shifted.

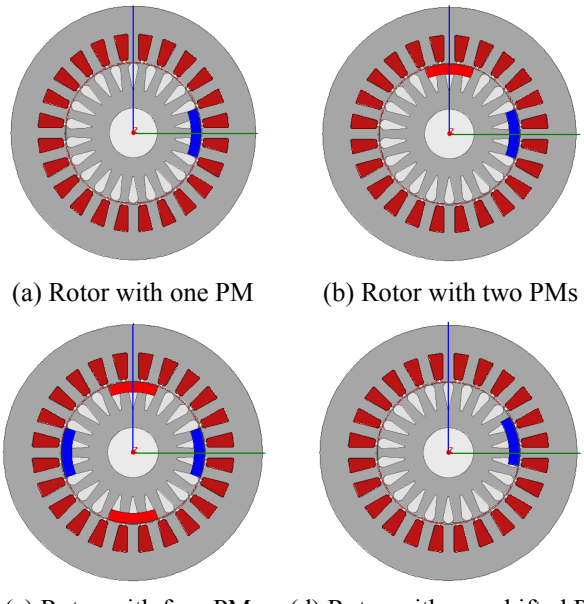

(a) Rotor with one PM (b) Rotor with two PMs

(c) Rotor with four PMs (d) Rotor with one shifted PM

Fig. 2. Cross section of LSPMSM with different rotor

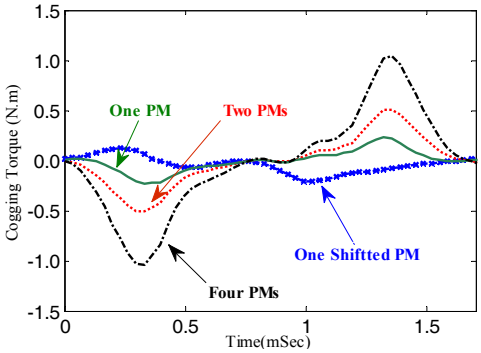

Fig. 3. Cogging torque for different rotor model

Therefore in a motor with 4 poles which are symmetrically distributed on a rotor with 24 stator slots, the overall cogging torque is four times the contribution of each pole. By setting an asymmetrical magnet distribution the periodicity and the additive effect both will be eliminated. By selection of appropriate angle shift between the magnets, the cogging torque can be decreased substantially [15].

The total cogging torque depends on whether the number of slots per pole is an integer number or not [14]. For integer number of slots per pole the cogging torque of each magnet is in phase and the total cogging torque can be calculated as:

$$T_{cog} = N_p T_{cog_p} = N_p \sum_{k=1}^{\infty} T_{pkN_s} \sin(kN_s\theta) \tag{6}$$

For fractional number of slots per pole, magnets face different arrangements of slots and therefore the cogging torque contribution from the magnets are out of phase with each other which results in overall reduction of the cogging torque. In this situation the magnets of the machine can be divided in several groups. The cogging torque generated by magnets in one group is out of phase with each other meanwhile the cogging torque contributed from each group is in phase with cogging torque from other groups. The number of groups in a machine is equal to the Greatest

Common Divisor (GCD) between the number of poles N_p and the number of stator slots N_s:

$$m = GCD(N_p, N_s) \tag{7}$$

The number of poles in each group can be obtained from:

$$\gamma = \frac{N_p}{m} \tag{8}$$

It is worth noting that the number of cogging torque cycles in a slot pitch rotation is equal to γ. Therefore the frequency of cogging torque in one mechanical rotation is γN_s which is equal to the least common multiple of N_p and N_s. The total cogging torque can be derived as follows:

$$T_{cog} = m T_{cog_g} = N_p \sum_{k=1}^{\infty} T_{pk\gamma N_s} \sin(k\gamma N_s\theta) \tag{9}$$

3. Magnet Shifting Method

As described in previous section, the cogging torque generated by one PM and the total cogging torque can be represented by summation of series of harmonics. If magnets are being shifted by an appropriate angle, the harmonic components of cogging torque will start cancelling each other and as a result the overall cogging torque will be reduced due to this magnets shifting. As the approach will be different depending on the number of slots per pole (integer versus fractional number of slots per pole), each configuration will be discussed separately.

3.1 Integer number of slots per pole

For integer number of slots per pole, every two adjacent magnets are selected as a group [21]. In each group one of the magnets is shifted relative to the other magnet by angle θ_0 as shown in Fig. 4. In this case the cogging torque can be written as following equation:

$$T_{cog} = \frac{N_p}{2} \sum_{k=1}^{\infty} T_{pkN_s} \begin{bmatrix} \sin kN_s\theta + \\ \sin kN_s(\theta - \theta_0) \end{bmatrix} \tag{10}$$

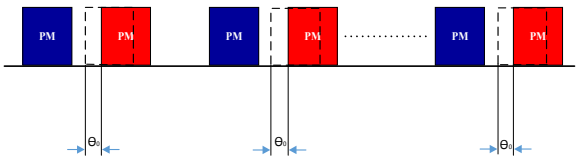

Fig. 4. Schematic diagram of shifting magnets

In which the shift angle can be described as:

$$\theta_0 = \frac{\pi}{N_s} \tag{11}$$

By simplification the cogging torque can be calculated as:

$$T_{cog} = N_p \sum_{k=1}^{\infty} T_{p2kN_s} \sin(2kN_s\theta) \tag{12}$$

It can be seen from Eq. (12) that the odd harmonics containing the fundamental harmonic of cogging torque are eliminated, which results substantial reduction of cogging

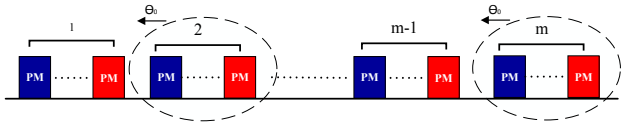

Fig. 5. Schematic diagram of shifting group of magnets

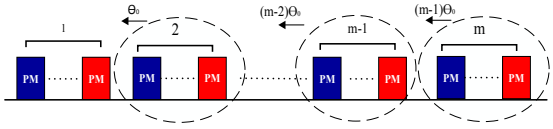

Fig. 6. Schematic diagram of shifting group of magnets

torque.

3.2 Fractional number of slots per pole

For fractional number of slots per pole the approach will be slightly different depending on whether the number of groups (m) is an even or an odd number.

If the number of groups is an even number, every two adjacent groups are selected as a new group. Then in each new group which consists of two sub-groups, one sub-group is being shifted relative to other sub-group by angle θ_0. As shown in Fig. 5. In this case the resulting cogging torque can be written as follows:

$$T_{cog} = \frac{m\gamma}{2}\sum_{k=1}^{\infty} T_{pk\gamma N_s}\begin{bmatrix}\sin k\gamma N_s\theta + \\ \sin k\gamma N_s(\theta-\theta_0)\end{bmatrix} \tag{13}$$

The shift angle can be described as:

$$\theta_0 = \frac{\pi}{\gamma N_s} \tag{14}$$

And the resulted cogging torque can be simplified as following equation:

$$T_{cog} = N_p\sum_{k=1}^{\infty} T_{p2k\gamma N_s}\sin(2k\gamma N_s\theta) \tag{15}$$

Eq. (15) shows the cancelling effect on the fundamental frequency γN_s and odd harmonics that cause reduction of cogging torque.

For odd group numbers one group is selected as fixed and the rest of the groups will be shifted relative to the fixed group by angle $\theta_0, 2\theta_0, \cdots, (m-1)\theta_0$, respectively as shown in Fig. 6, In this case the resulting cogging torque can be described as:

$$\begin{aligned} T_{cog} &= \sum_{i=1}^{m} T_{cog_{g_i}} \\ &= \sum_{h=0}^{m-1}\gamma\sum_{k=1}^{\infty} T_{pk\gamma N_s}\sin k\gamma N_s(\theta - h\theta_0) \end{aligned} \tag{16}$$

In which the shift angle can be described as:

$$\theta_0 = \frac{2\pi}{N_s N_p} \tag{17}$$

And the cogging torque can be derived from Eq. (18) as:

$$T_{cog} = N_p\sum_{k=1}^{\infty} T_{pkN_sN_p}\sin(kN_sN_p\theta) \tag{18}$$

From Eq. (18) it can be concluded that the fundamental frequency of the resulting cogging torque has increased to N_sN_p times per mechanical revolution. As a result by cancelling lower order high amplitude harmonics, cogging torque will be reduced significantly.

4. Numerical Results

Numerical results are calculated using the FEA by Ansoft's Maxwell 2D. The magnet shifting method presented in previous section is applied to a 4 pole 24 slot inset LSPMS motor with the parameters shown in Table 1. The machine has an integer number of slots per pole and as a result by using Eq. (11) the magnet shift angle is calculated as 7.5 degrees. By placing every two adjacent magnets in a group, each magnet is being shifted by 7.5 degree relative to the other magnet in the group, as shown in Fig. 7.

4.1. Cogging torque prediction

Cogging torque profile of the LSPMS motor with

Table 1. LSPMS Motor parameter

Stator outer diameter (mm)	125.4	Motor axial length(mm)	81
Stator inner diameter (mm)	70.3	Number of stator slots	24
Rotor inner diameter (mm)	24.5	Number of rotor bars	22
Air gap length (mm)	0.5	Number of poles	4
Stator slot depth (mm)	13.8	Pole arc(deg.)	41
Stator tooth width (mm)	7.6	Magnet thickness (mm)	5

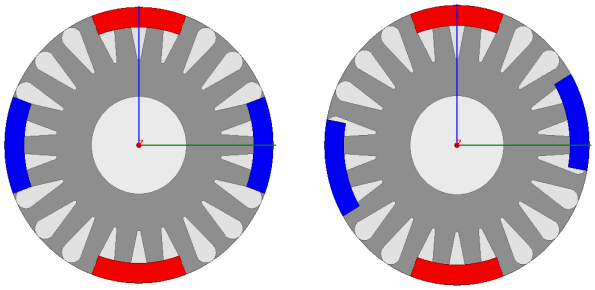

(a) Uniformly Distributed PMs (b) Shifted PMs

Fig. 7. Cross section of Inset LSPMSM rotor

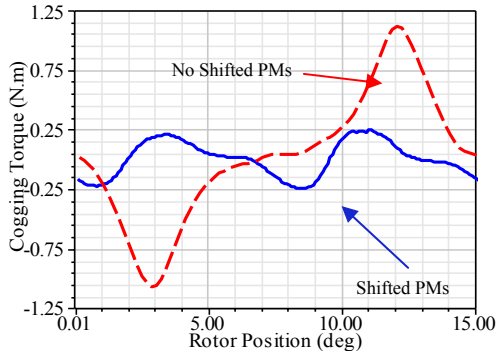

Fig. 8. Comparison of cogging torque profile

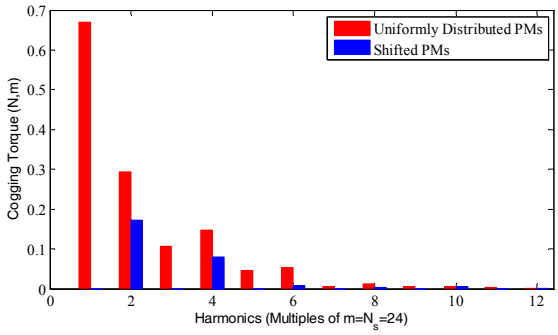

Fig. 9. Harmonic components of cogging torque

normal rotor and also cogging torque of the LSPMS motor with shifted PMs have been obtained from 2-D FEA and results are shown in Fig. 8 for comparison. As shown the peak to peak cogging torque for LSPMS motor with uniformly distributed magnet on the rotor is calculated as 2.19 N.m. This value for the LSPMS motor with shifted magnet rotor is calculated as 0.52 N.m which shows a reduction of 76% in cogging torque. The harmonic spectra of cogging torque for both motor are calculated using FFT (Fast Fourier Transform) algorithm by Matlab software and the results are presented in Fig. 9. The cancelling effect of shifting the magnets on cogging torque harmonics is clearly shown in the results, which is a verification of the theory discussed in previous section.

4.2 Magnet mmf distribution analysis

Application of shifting magnets deteriorates the symmetrical distribution of magnets mmf in the air gap and produces extra harmonics in the spectra. As a result, the effect of mmf harmonic components due to magnet shifting on back EMF, electromagnetic torque and iron loss should be investigated and considered in the approach. By assuming a rectangular magnet mmf distribution in the air gap, the rotor mmf distribution can be presented as shown in Fig. 10. The distributed mmf Fourier series and their coefficients can be calculated as:

$$F_g = \sum_{k=1}^{\infty} b_k \sin k\left(\frac{p}{2}\right)\theta \tag{19}$$

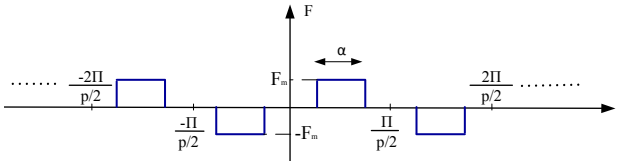

Fig. 10. Magnet mmf distribution in the air gap

$$b_k = \frac{4F_m}{\pi k}\sin\frac{k\pi}{2}\sin k\left(\frac{p}{2}\right)\left(\frac{\alpha}{2}\right) \tag{20}$$

Where α is the mechanical pole face arc. Therefore for a 4 pole motor the Fourier series of distributed mmf and their coefficients can be calculated as:

$$F_g = \sum_{k=1}^{\infty} b_k \sin(2k\theta) \tag{21}$$

$$b_k = \frac{4F_m}{\pi k}\sin\frac{k\pi}{2}\sin(k\alpha) \tag{22}$$

As shown in Eq. (22) only the odd harmonics of fundamental frequency are appearing in the distributed mmf. For a p-pole rotor with magnets as described in section 3.1, the Fourier series of mmf distribution in the air gap can be derived as follows:

$$F_g = \sum_{k=1}^{\infty} a_k \cos k\left(\frac{p}{2}\right)\theta + \sum_{k=1}^{\infty} b_k \sin k\left(\frac{p}{2}\right)\theta \tag{23}$$

In which the coefficients can be calculated as follows:

$$a_k = \frac{2F_m}{\pi k}\left(\sin k\left(\frac{p}{2}\right)\left(\frac{\alpha}{2}\right)\right)\times \left[\cos\frac{k\pi}{2} - \cos\left(\frac{3k\pi}{2} - k\frac{p}{2}\theta_0\right)\right] \tag{24}$$

$$b_k = \frac{2F_m}{\pi k}\left(\sin k\left(\frac{p}{2}\right)\left(\frac{\alpha}{2}\right)\right)\times \left[\sin\frac{k\pi}{2} - \sin\left(\frac{3k\pi}{2} - k\frac{p}{2}\theta_0\right)\right] \tag{25}$$

Where θ_0 is the shift angle of magnets. Thus for a 4 pole shifted magnet motor the mmf Fourier series and their coefficient can be calculated as:

$$F_g = \sum_{k=1}^{\infty} a_k \cos 2k\theta + \sum_{k=1}^{\infty} b_k \sin 2k\theta \tag{26}$$

$$a_k = \frac{2F_m}{\pi k}\sin k\alpha\left[\cos\frac{k\pi}{2} - \cos\left(\frac{3k\pi}{2} - 2k\theta_0\right)\right] \tag{27}$$

$$b_k = \frac{2F_m}{\pi k}\sin k\alpha\left[\sin\frac{k\pi}{2} - \sin\left(\frac{3k\pi}{2} - 2k\theta_0\right)\right] \tag{28}$$

As shown in Eq. (26) there are odd and even harmonics

Table 2. Magnet mmf distribution harmonics

Harmonic Number	Uniformly Distributed PMs	Shifted PMs Rotor
1	1.0	0.99
2	0.0	0.19
3	0.43	0.39
4	0.0	0.05
5	0.13	0.10
6	0.0	0.16
7	0.21	0.12
8	0.0	0.08
9	0.02	0.01
10	0.0	0.11

of fundamental frequency in mmf distribution in this case. A comparison between the harmonic contents of magnet mmf distribution in the air gap for two cases of uniformly distributed PMs and shifted PMs rotor are shown in Table 2 for 1st up to 11th harmonic.

4.3 Phase back EMF analysis

The phase back-EMF waveforms for both normal rotor and shifted magnet rotor have been obtained using finite element simulation and the results are depicted and compared in Fig. 11. The harmonic spectra of back EMF of both motors are calculated using FFT algorithm by Matlab software and the results are presented in Fig. 12. As shown the fundamental component of back EMF remains almost unchanged while the other harmonics containing tripplen and belt harmonics are reduced which was expected due to the effect of magnet shifting on PM mmf distribution. analysis described in previous section. The results show that the back EMF phase voltage Total Harmonic Distortion (THD) for LSPMS motor with uniformly distributed magnet on rotor is 36.3%. For the shifted magnet rotor back EMF phase voltage THD is calculated as 28.1%. This result verifies that less distorted back EMF is achieved in motor with shifted PMs. It is worth noting that the induced voltages due to even harmonics in two sides of a coil are in phase and therefore in the coil voltage cancel each other. The tripplen harmonics in a three phase machine are normally eliminated by the phase connection.

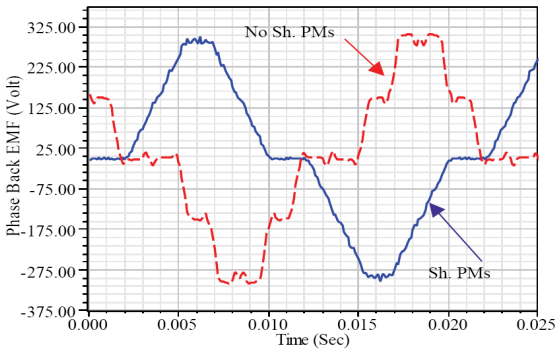

Fig. 11. phase back EMF waveform

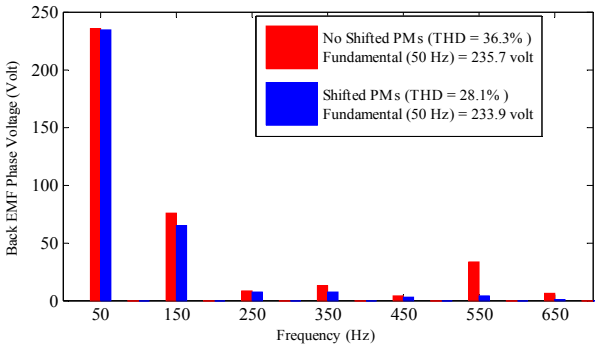

Fig. 12. Phase back EMF harmonic contents

4.4 Electromagnetic torque

Cogging torque and back EMF harmonics are well known causes for toque ripple in the developed electro-magnetic torque. As described before the method of magnet shifting not only reduces the cogging torque but also improves the back EMF harmonic spectra, and therefore the torque quality is expected to improve. In order to verify this statement, two LSPMS motors are being selected for study. One with normal rotor and the other one with shifted magnet rotor (as described before). Motors are supplied with nominal three phase balanced voltage and a mechanical fan load of ($T_l = 2.54*10^{-4}\omega^2$) is applied to them. The moving torque generated by the two motors are obtained by FEA and the results are shown in Fig. 13 for comparison. As shown in Fig. 13 the torque ripple index is reduced by approximately 50% when Magnet Shifting is implemented. Therefore the torque performance of LSPMS motors will be improved substantially with application of Magnet Shifting.

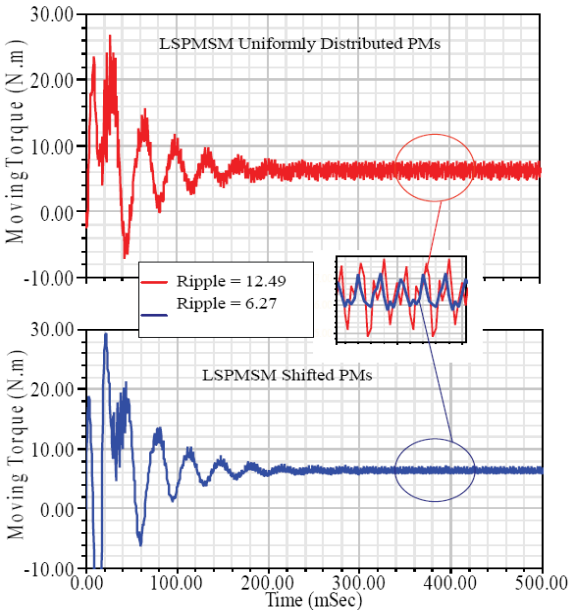

Fig. 13. Comparison of torque derived by FEA

4.5 Core losses

Loss calculation is of particular importance in order to accurately anticipate the efficiency and thermal limitation of a machine during design and optimization stages. Under sinusoidal flux condition, core loss can be divided into three components: hysteresis loss P_h, eddy current loss P_c and excessive loss (or anomalous) P_e. According to the Steinmetz equation the specific core loss P_v in watts per kilogram can be expressed as:

$$p_v = k_h f B_m^2 + k_c (f B_m)^2 + k_e (f B_m)^{1.5} \quad (29)$$

Where K_h is the hysteresis coefficient, K_c is the classical eddy coefficient, K_e is the excess or anomalous eddy current coefficient due to magnetic domain, B_m is the maximum amplitude of the flux density and f is the frequency of exciting voltage [22]. As previously indicated magnet shifting deteriorates magnet mmf distribution symmetry in the air gap and produces extra harmonics in mmf and magnetic flux density spectra. It is known that core loss coefficients are variable and their values depend on both magnetic flux density and frequency [23]. Typical conventional core loss models which are based on constant coefficients are not accurate. In order to accurately predict the core loss, variable loss coefficients should be incorporated in the model. Transient 2-D FEA can be used to calculate the core loss in electrical steel laminations considering flux harmonics. The core loss coefficients are calculated from multiple core loss curves provided in the form of total loss versus flux density in different frequencies. The core losses in both stator and rotor laminations for motor with normal rotor and motor with shifted magnet rotor are calculated and depicted in Fig. 14. Comparison between the two LSPMS motors show that by shifting magnets the core loss is slightly increased.

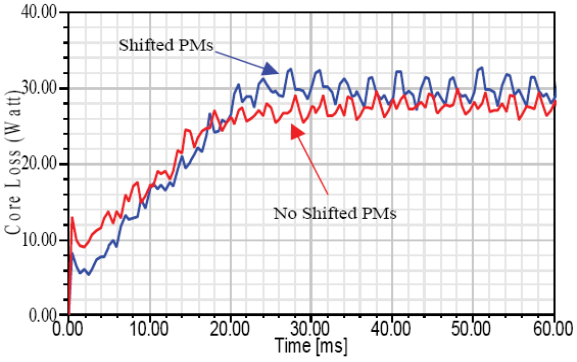

Fig. 14. Core loss from FEA

5. Experimental Results

In order to validate the numerical results two prototype LSPMS motors are selected based on parameters shown in

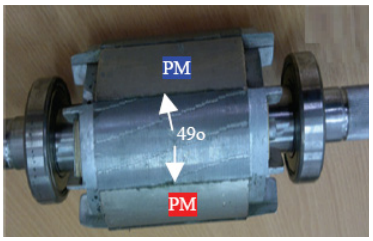

(a) No Shifted PMs

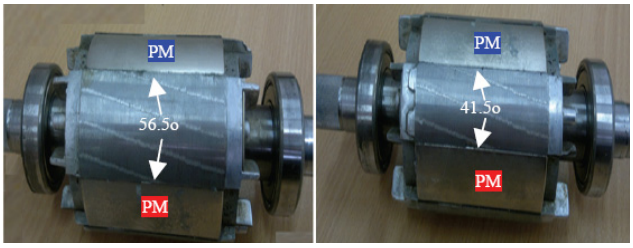

(b) Shifted PMs

Fig. 15. Prototype rotors of LSPMS motors.

Table 1. The main difference between the two motors is the distribution of PMs on their rotors. One motor has a uniformly distributed PMs and the other one has shifted PMS as shown in Fig. 15.

5.1 Cogging torque measurement

LSPMS motor and the cogging torque measurement setup are shown in Fig. 16. In order to measure cogging torque, a rotating index plate is assembled onto the worm-gear unit. The rotating index plate can turn and hold the stator securely with accurate angular position. The rotor position is being kept stationary during the measurements. One end of a balanced beam is attached to the rotor shaft and the other end is being placed on the tray of a digital weight gauge (as shown in Fig. 16). With the beam in a level position, the weight gauge is set to zero. In order to allow measurement of both positive and negative values of cogging torque, a pre load is added to the measurement end to ensure that the bar is always in contact with the tray. As the stator is turned in the lathe, the relative position between the rotor and the stator is changed. By reading the measured force the resulted cogging torque can be calculated as follows [24].

$$T_{cog} = L.(F_{read} - F_{pre-load}) \quad (30)$$

In which L is the arm length of the balanced beam from the center of rotor shaft to the acting point on the digital gauge. F_{read} and $F_{pre-load}$ are the weight reading from the digital gauge and the pre load weight in Newton. One cogging torque period for normal rotor and two cogging torque periods for shifted PMs rotor were generated by the index plate. Total of 15 samples per

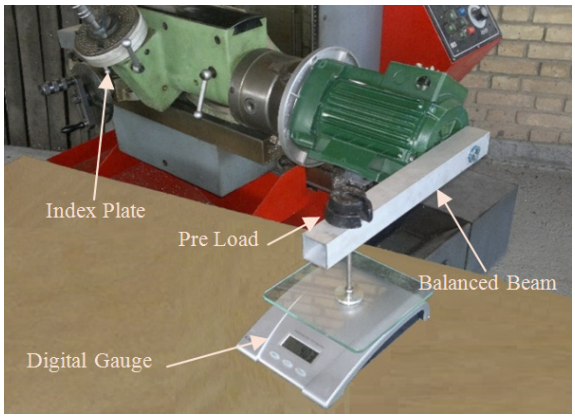

Fig. 16. Cogging torque measurement setup

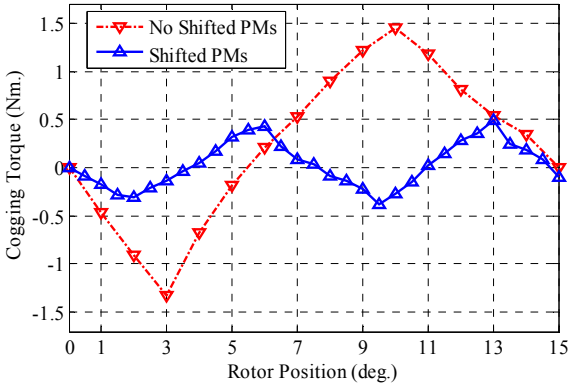

Fig. 17. Cogging torque profiles from experimental approach

period were taken for each machine.

The cogging torque profiles from experimental test for both motors are shown in Fig. 17. The experimental results can be compared with the results obtained from 2-D FEA models in Fig. 8. The peak to peak cogging torque for motor with uniformly distributed magnets is measured as 2.75 N.m from the experiment. This value is obtained as 0.8 N.m for the shifted magnet rotor which indicates a 71% reduction in cogging torque. Generally in a laboratory prototype, some of the mechanical tolerances cannot be fully calibrated. Considering the measurement errors in the test and sensitivity of the cogging torque to the machine parameters, it can be concluded that the cogging torque results are in satisfactory agreement with the simulation results.

5.2 Phase back EMF measurement

For the back EMF tests, a dc motor is used to drive the rotors of the LSPMS motors at the rated speed as shown in Fig. 18. The phase back EMF waveform for both normal motor and shifted magnet motor derived by experimental approaches are illustrated in Fig. 19. The phase back EMF waveforms of the two prototypes measured at 1500 rpm can be compared with the 2-D FEA results were presented in Fig. 11. In order to validate the numerical results the harmonic spectra of measured back EMF of both motors are calculated using FFT algorithm by Matlab software and by using the Excel files provided by the oscilloscope. The results are shown in Fig. 20 and can be compared with the 2-D FEA results in Fig. 12. The results show that the

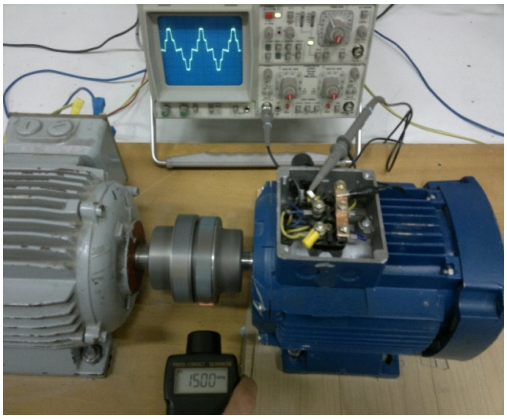

Fig. 18. Experimental test bench for back EMF measurement

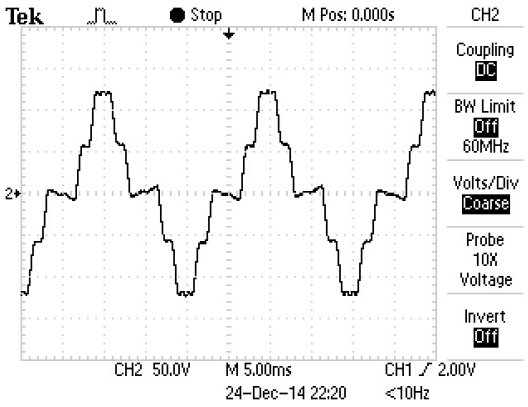

(a) Uniformly distributed PMs Rotor

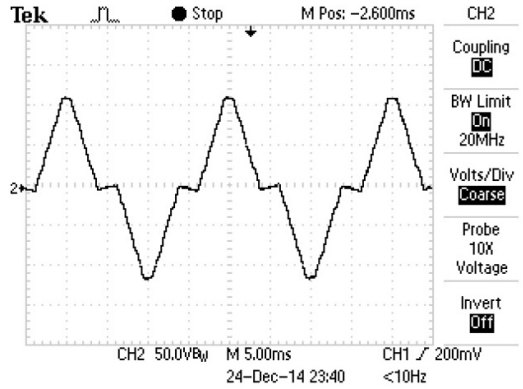

(b) Shifted Rotor PMs

Fig. 19. Phase back EMF profiles from experimental approach

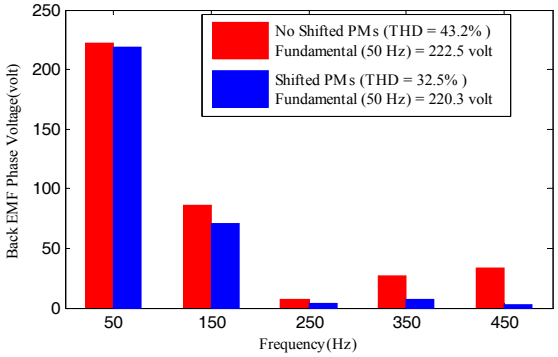

Fig. 20. Harmonic components of measured Phase back EMF

measured back EMF phase voltage THD for LSPMSM with uniformly distributed magnet on rotor is 43.2%. This value is calculated as 32.5% for the shifted magnet motor. This indicates less distorted back EMF voltage in shifted PMs motor which verify the results from 2-D FEA. Since measurement of voltage is normally less sensitive to mechanical deficiency of the machine and the experimental errors as compared to cogging torque measurement, there are excellent agreements between the simulated and measured results.

5.3 Core loss measurement

In order to measure core loss of the two prototype LSPMS motors some tests should be done as follows. Before assembling the magnets, two prototype motors can be considered as induction motors. According to IEEE Std 112-2004 the friction and windage loss can be determined for two motors [25].

As we expected the test results showed that the friction and windage loss for both motors were almost equal. The friction and windage loss value obtained from the tests was about 18.5 watt. After assembling the magnets, the no-load test was performed by running the machine as a motor at rated voltage and frequency with no connected load. The measured input power is the total losses in the motor at no-load. These losses consist of the stator copper loss, friction, windage and core losses. The core loss is obtained by subtracting the value of windage and friction loss from the input power minus stator copper loss. These tests have been done for two prototype motors. For LSPMSM with normal rotor the value of core loss was obtained about 30.5 watt. For LSPMSM with shifted magnet rotor the value of core loss was obtained about 33.8 watt. The test results showed that by shifting magnets the core loss is slightly increased which verifies the numerical results obtained in section 4.3.

5.4 Load test

In order to investigate the effect of magnet shifting on motor performance under load, a load test was performed. Test load is performed for determination of current, power factor, speed and efficiency. As shown in Fig. 17, a DC generator with resistive load was coupled with the prototype motor as a mechanical load. The LSPMS motors have been connected to a balanced supply at rated voltage and frequency. The LSPMSM load has been increased by increasing DC generator load. The test results for LSPMS motor with normal rotor and LSPMS motor with shifted magnet rotor at rated load have been shown in Table 3.

Table 3. LSPMS Motor parameters at rated Load

LSPMS Motor	Normal Rotor	Shifted PMs Rotor
Vs (v)	220	220
I s (A)	1.83	1.9
Pin (Watt)	1174	1170
Pout(Watt)	1044	1036
COS ϕ	0.97	0.93
ϕ	0.889	0.885
N(rpm)	1500	1500

V_s is the stator phase voltage, I_s is the stator line current, P_{in} and P_{out} are three phase input and output power respectively, $\cos\phi$ is the power factor, η is the efficiency and N is the rotor speed. The comparison between values in the table shows the motor efficiency has no noticeable change due to magnet shifting.

6. Conclusion

This paper presents a magnet shifting method for cogging torque reduction in inset LSPMS motors. The method is applied to a 4 pole inset LSPMS motor and the results compared with the results of FEA. This study shows that the proposed technique can reduce the cogging torque and the torque ripple very effectively. FEA results also show that by application of magnet shifting, the fundamental component of back EMF remains almost unchanged but other harmonics containing tripplen and belt harmonics are reduced. Therefore less distorted back EMF voltage is achieved by the method.

Experimental tests have been conducted for machines with two rotor configurations to validate the FEA models and the proposed method. The results showed that the magnet shifting method is an effective approach for reduction of cogging torque in LSPMS motors. The phase back EMF waveforms of the motors were also obtained from the experiment and FEA results and the comparison showed that good agreement exists between the two results. The numerical and experimental results also show that the proposed shifting magnet method in this paper increases the core losses slightly. Also the load test shows that by magnet shifting the motor efficiency has no noticeable change.

References

[1] A.T. De Almeida, F.J.T. E. Ferreira, and C. Fong, "*Standards for efficiency of electric motors*, " IEEE Industry Applications Magazine, Jan.-Feb. 2011.

[2] W. Fei, P. C. K. Luk, J.Ma, J. X. Shen, and G. Yang, "*A High-Performance Line-Start Permanent Magnet synchronous motor Amended From a Small Industrial Three-Phase Induction motor*," IEEE Transaction on Magnetics, Vol. 45, No. 10, October 2009.

[3] Qiping Chen, Hongyu Shu and Limin Chen, "*Simulation analysis of cogging torque of permanent magnet synchronous motor for electric vehicle*," Journal of Mechanical Science and Technology, 26 (12) (2012), 4065~4071, Springer.

[4] Claudio Bianchini, Fabio Immovilli, Emilio Lorenzani, Alberto Bellini, and Matteo Davoli, "*Review of Design Solutions for Internal Permanent-Magnet Machines Cogging Torque Reduction*," IEEE Transaction on Magnetics, V0l. 48, N0. 10, October 2012.

[5] Li Zhu, S. Z. Jiang, Z. Q. Zhu, C. Chan, "*Analytical Methods for Minimizing Cogging Torque in Permanent-Magnet Machines*," IEEE Transactions on Magnetics, Vol. 45, N0. 4, April 2009.

[6] Z. J. Liu and J. T. Li, "*Analytical Solution of Air-Gap Field in Permanent-Magnet Motors Taking Into Account the Effect of Pole Transition Over Slots*," IEEE Transactions on Magnetics, Vol. 43, No. 10, October 2007.

[7] Nicola Bianchi and Silverio Bolognani, "*Design Techniques for Reducing the Cogging Torque in Surface-Mounted PM Motors*," IEEE Transactions on Industry Applications, Vol. 38, No. 5, September/ October 2002.

[8] D. C. Hanselman, "*Effect of skew, pole count and slot count on brushless motor radial force, cogging torque and back EMF*," Proc. Inst Elect. Eng., vol. 144, no. 5, pp. 325-330, 1997.

[9] R. Islam, I. Husain, A. Fardoun, and K. McLaughlin, "*Permanent-Magnet Synchronous Motor Magnet Designs With Skewing for Torque Ripple and Cogging Torque Reduction*," IEEE Transactions on Industry Applications, Vol. 45, No. 1, Jan.-Feb. 2009.

[10] Sang-Moon Hwang, Jae-Boo Eom, Yoong-Ho Jung, Deug-Woo Lee, and Beom-Soo Kang, "*Various Design Techniques to reduce Cogging Torque by Controlling Energy Variation in Permanent Magnet Motors*," IEEE Transactions on Magnetics, Vol. 37, No.. 4, July 2001.

[11] Z. Q. Zhu and David Howe, "*Influence of Design Parameters on Cogging Torque in Permanent Magnet Machines*," IEEE Transactions on Energy Conversion, Vol. 15, No. 4, December 2000.

[12] Z. Q. Zhu, S. Ruangsinchaiwanich, N. Schofield, and D. Howe, "*Reduction of Cogging Torque in Interior-Magnet Brushless Machines*," IEEE Trasactions on Magnetics, Vol. 39, No. 5, September 2003.

[13] Takeo Ishikawa, Gordon R. Slemon, "*A Method of Reducing Ripple Torque in Permanent Magnet Motors without Skewing*," IEEE Tranactions on Magnetics, Vol. 29, No. 2, March 1993.

[14] Luke Dosiek, Pragasen Pillay, "*Cogging Torque Reduction in Permanent Magnet Machines*," IEEE Transaction on Industry Applications, Vol. 43, No. 6, Nov.-Dec. 2007.

[15] C. Bretón, J. Bartolomé, J. A. Benito, G. Tassinario, I. Flotats, C. W. Lu, and B. J. Chalmers, "*Influence of Machine Symmetry on Reduction of Cogging Torque in Permanent-Magnet Brushless Motors*," IEEE Transaction on Magnetics, Vol. 36, No. 5, September 2000.

[16] S. M. Hwang, J. B. Eom, G. B. Hwang, W. B. Jeong, and Y. H. Jung, "*Cogging torque and acoustic noise reduction in permanent magnet motors by teeth paring,*" IEEE Transaction on Magnetics, vol. 36, No. 5, Sep. 2000.

[17] R. Lateb, N. Takorabet, and F. Meibody-Tabar, "*Effect of magnet segmentation on the cogging torque in surface-mounted permanent magnet motors*," IEEE Transaction on Magnetics, vol. 42, No. 3, Mar. 2006.

[18] Abolhassan Ghasemi, "*Cogging Torque Reduction and Optimization in Surface mounted Permanent Magnet Motor Using Magnet Segmentation Method*," Electric Power Components and Systems, Taylor & Francis Group 42:1239-1248, 2014

[19] Tiberiu Tudorache and Ion Trifum, "*Permanent-Magnet Synchronous Machine Cogging Torque Reduction Using a Hybrid Model*," IEEE Transaction on Magnetics, vol. 48, No. 10, October 2012.

[20] D. Hanselman, "*Brushless Permanent-Magnet Motor Design*," New York McGraw-Hill, pp 117-121, 1994

[21] Ting Liu, Shoudao Huang, Jian Gao, "*A Method for Reducing Cogging Torque by Magnet Shifting in Permanent Magnet Machines*," International Conference on Electrical Machines and Systems(ICEMS), 2010.

[22] Dan M. Ionel, Mircea Popescu, Stephen J. Dellinger, T. J. E. Miller, Robert J. Heideman, and Malcolm I. McGilp, "*On the Variation With Flux and Frequency of the Core Loss Coefficients in Electrical Machines*," IEEE Transaction on Industry Appli-cations, Vol. 42, No. 3, May/June 2006.

[23] N. Ozturk and E. Celik, "*Application of Genetic Algorithms to Core Loss Coefficient Extraction*," Progress In Electromagnetic Research, Vol. 19, 133-146, 2011.

[24] Z.Q. Zhu, "*A Simple Method for Measuring Cogging Torque in Permanent Magnet Machines*," Power and energy Society General Meeting, 2009.PES'09, IEEE.

[25] IEEE Std 112TM -2004, "*IEEE Standard Test Procedure for Polyphase Induction Motors and Generators*"

Hamidreza Behbahanifard He received B.S and M.Sc. degree in power engineering from Isfahan University of Technology, Isfahan, Iran and Sharif University of Technology, Tehran, Iran respectively. Currently he is a PhD candidate in power engineering in Malek Ashtar University of Technology, Isfahan, Iran. His research interests include electrical machine analysis and design, condition monitoring and fault diagnosis of electric machines and rotating systems.

Alireza Sadoughi He received the B.S. and M.S. degrees in electrical engineering from Tehran University, and also Ph.D. degree in electrical engineering from Isfahan University of Technology. His research interests include electrical machines analysis and design, electrical drives, condition monitoring and fault diagnosis of electric machines and rotating systems, simulation techniques in electrical machines, and renewable energy systems and installations.